Fluorinated Aromatic Monomers as Building Blocks to Control α-Peptoid Conformation and Structure

Diana Gimenez,[†] Guangfeng Zhou,[‡] Matthew F. D. Hurley,[‡] Juan A. Aguilar,[†] Vincent A. Voelz*,[‡] and Steven L. Cobb*,[†]

[†] Durham University, Department of Chemistry, South Road, Durham, DH1 3LE, U.K.

[‡] Temple University, Department of Chemistry, Philadelphia, Pennsylvania 19122, U.S.

Supporting Information Placeholder

ABSTRACT: Peptoids are peptidomimetics of interest in the fields of drug development and biomaterials. However, obtaining stable secondary structures is challenging and designing these requires effective control of the peptoid tertiary amide *cis*/*trans* equilibrium. Herein, we report new fluorine containing aromatic monomers that can control peptoid conformation. Specifically, we demonstrate that a fluoropyridine group can be used to circumvent the need for monomer chirality to control the *cis*/*trans* equilibrium. We also show that incorporation of a trifluoro-methyl group (*N*^{CF3}Rpe) rather than a methyl group (*N*Rpe) at the α-carbon of a monomer gives rise to a 5-fold increase in *cis*-isomer preference.

α-Peptoids (**Figure 1a**) are resistant to protease degradation[1] and are thermally stable.[2] They are of interest as therapeutics[1,3–8] and as biomaterials.[9] However, because a peptoid is composed of *N*-alkyl amide bonds, there is no capacity to use hydrogen bonding to stabilize folded structures. Accessing and designing stable structures, such as helices,[10–13] ribbons,[14] loops[15] or sheets[16,17] relies on utilizing a limited number of peptoid monomers that can predictably restrict the amide bond isomerism. An early advance was reported by Zuckermann and Barron, who showed that monomers with *N*-α-chiral aromatic side-chains, such as *N*Spe (**2**)(**Figure 1b**), can stabilise all *cis*-amide polyproline I helices (PPI).[10,18] Gorske and Blackwell explored non-covalent interactions (NCI) including sterics, hydrogen bonding and electronic $n\rightarrow\pi^*$ effects to control the *cis*/*trans* equilibrium in model peptoid systems, through which they identified new chiral peptoid monomers such as *N*S1npe (**3**) and *N*Sfe (**4**) (**Figure 1b**), able to impose larger $K_{cis/trans}$ values than *N*Spe (**2**).[19–21] Monomers such as **3** and **4** exert their effects through a synergystic combination of steric factors (e.g. α-methylation) and electronic $n\rightarrow\pi^*_{Ar}$ interactions. While all of the aforementioned monomers are neutral, pioneering work by Taillefumier and Faure demonstrated that positively charged triazolium-type monomers impart an impressive level of conformational control into a peptoid backbone.[22] Yet, while this approach gives some of the largest $K_{cis/trans}$ values reported, the use of charged monomers puts restrictions on designed peptoid sequences.

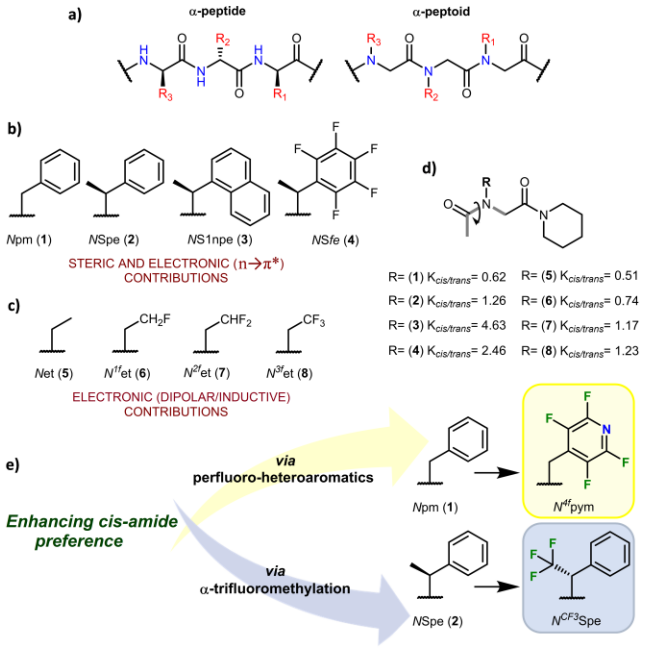

Figure 1. a) α-peptides and α-peptoids; **b**) *cis*-amide preference due to steric and $n\rightarrow\pi^*$ electronic effects (**2-4**); **c**) *cis*-amide preference due to inductive effects (**5-8**); **d**) $K_{cis/trans}$ (CD_3OD) for monomers **1-8**; **e**) Application of fluorine to enhance *cis*-isomer preference.

While some work has been carried out to exploit fluorine in the design of new peptoid monomers (e.g. *N*Sfe, **4**), we sought to investigate the application of perfluoro-heteroaromatics, such as tetrafluoropyridine. We hypothesized that such highly electron-deficient systems would favor even stronger $n\rightarrow\pi^*_{Ar}$ interactions, overcoming the need for monomer chirality. To investigate this hypothesis, three model di-peptoids based on the non-chiral benzylamine (*N*pm, **1**), pyrinidylmethanamine (*N*pym, **9**), and (tetrafluoropyrinidyl)methanamine (*N*^{4f}pym, **10**) were prepared for conformational analysis (**Figure 2b**).

We recently reported that fluorine atom(s) β to the amide bond nitrogen promote enhanced *cis*-amide preference in

non-chiral alkyl type monomers (**Figure 1c**).[23] This *cis*-amide preference was found to rely on fluorine induced dipolar interactions. Following this we envisaged that incorporation of a trifluoromethyl (CF_3) group into an aromatic monomer might allow both electronic (dipolar interactions) and steric effects to be utilized in tandem to access systems in which the *cis*/*trans* equilibrium completely favors one isomer. To explore this, we prepared the α-trifluoromethyl (N^{CF_3}Rpe) model peptoid **12** (**Figure 2c**). For comparison, the non-fluorinated reference **11** was also prepared. The synthetic route employed to model peptoids (**1, 9-12**) is shown in **Figure 2a**.[20,21]

We employed ^{1}H-NMR and ^{1}H-^{1}H-NOESY to evaluate the *cis*/*trans* ratios present within the model systems (see SI for further details).[24,20,21] Analysis of **1** showed that, as reported, the benzyl side-chain induces a solvent dependent conformational preference (**Figure 2d**).[21] In $CDCl_3$, a *trans*-amide geometry is favored by 0.79 kcal mol^{-1}, while in more polar solvents no conformation preference was found (e.g. ΔG~0 in both CD_3CN and CD_3OD, **Figure 2d**). Replacement of the aromatic ring with a hetero-aromatic group caused a significant increase in the *cis*-isomer preference seen across all of the solvents tested (**1** *versus* **9** in **Figure 2d**). When the electron-withdrawing character of the aromatic ring was further increased, through the incorporation of a tetrafluoropyridine group (N^{4f}pym), an impressive increase in the $K_{cis/trans}$ values was seen (**10** in **Figure 2d** and **Figure 3**). Indeed, **10** showed a 3-fold higher $K_{cis/trans}$ value in $CDCl_3$ than its non-fluorinated analogue **9** ($K_{cis/trans}$= 1.41 vs. 0.47, **Figure 3**). The conformational preference of **10** was enhanced in polar solvents where highly biased *cis*-populations were seen ($K_{cis/trans}(CD_3CN)$= 3.22, 76% *cis*-isomer; $K_{cis/trans}(CD_3OD)$= 2.22, 69% *cis*-isomer content; **Figure 2d**). Interestingly, analysis of the NOE correlations within **10** implied that the fluoro-pyridine ring sits facing the N-terminal carbonyl group in the *cis*-isomer (**Figure 3**). This result supports a mechanism in which the *cis* conformation is stabilized by means of fluorine enhanced $n\rightarrow\pi^*_{Ar}$ interactions. The $K_{cis/trans}$ values recorded for **10** are among the highest ever reported for a neutral non-chiral monomer in this type of peptoid model system. What is more remarkable is that despite being a non-chiral monomer, the *cis*-isomer preferences induced by N^{4f}pym are comparable or even greater than those produced by the widely utilized α-chiral monomers such as **2** and **4** (**Figure 2b** and **Figure 2d**).

We then turned our attention to the effects imparted by fluorine at the α-methyl position. The results obtained for the reference (**11**) agreed fully with those previously reported for the (*S*)-enantiomer (NSpe, **2**) (**Figure 2d**).[21] **11** exhibited almost no conformational preference in $CDCl_3$ ($K_{cis/trans}$ ~ 1.0). Again, in line with the literature, in polar solvents its *cis*/*trans* equilibrium shifted in favour of the *cis*-isomer, particularly in CD3CN ($K_{cis/trans}$= 2.07).[21] In stark contrast, however, the N^{CF_3}Rpe containing di-peptoid **12** displayed a high degree of conformational preference. Both the ^{1}H and the ^{19}F NMR data of **12** revealed the presence of one isomer in solution with a predominance of ≥84% (**Figure 2d**). It was not possible to use ^{1}H-^{1}H NOESY correlations within **12** to assign the configuration of the major isomer present (e.g see Fig. S95). Therefore, to better understand the conformational preference exhibited by **12**, computational studies were performed using both *ab initio* QM and replica exchange

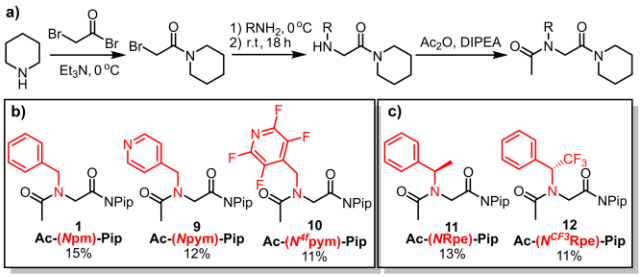

d)

Product	(CDCl3) $K_{cis/trans}$	(CDCl3) $^{AVG}\Delta G_{cis/trans}$ (kcal mol^{-1})	(CD3CN) $K_{cis/trans}$	(CD3CN) $^{AVG}\Delta G_{cis/trans}$ (kcal mol^{-1})	(CD3OD) $K_{cis/trans}$	(CD3OD) $^{AVG}\Delta G_{cis/trans}$ (kcal mol^{-1})
1	0.27±0.01	0.79±0.03	1.20±0.06	-0.11±0.03	0.71±0.03[a]	0.20±0.03[a]
9	0.46±0.01	0.45±0.02	1.66±0.06	-0.30±0.02	1.15±0.02	-0.08±0.01
10	1.41±0.16	-0.20±0.08	3.22±0.12	-0.69±0.03	2.22±0.04	-0.47±0.01
11	0.92±0.05	0.05±0.04	2.07±0.12	-0.43±0.04	1.35±0.04	-0.18±0.02
12[b][c]	5.17±1.25	-0.95±0.19	5.82±0.23	-1.04±0.03	6.41±0.13	-1.10±0.02

Figure 2. a) Synthesis of model peptoids; **b**) Non-chiral di-peptoids **1**, **9-10**; **c**) Chiral di-peptoids **11**, **12**. **d**) Average $K_{cis/trans}$ values for **1**, **9-12**. From each replica, $\Delta G = -RTLn(K_{cis/trans})$ at 25 ºC. Averages and SD values given for n=6; [a]n=5 and [b]n=3. [c]Major isomer assigned as *cis*, in agreement with MD data.

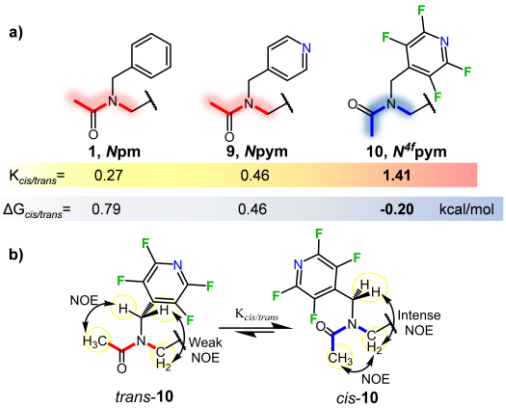

Figure 3. a) Amide bond geometry in systems **1**, **9** and **10**. **b**) Experimental ^{1}H-^{1}H NOESY correlations within *cis*/*trans* conformers of **10**. All $K_{cis/trans}$ values as determined in $CDCl_3$.

molecular dynamics (REMD).

Scans of side-chain and backbone dihedral angles were performed using DFT at the B3LYP/6-311G+(2d,p)//HF/6-31G(p) level of theory (**Figure 4**). To identify side-chain conformational minima, χ_1 and χ_2 angles were first scanned from 0° to 360° in 30° intervals starting from typical backbone conformations of peptoids: *cis*-amide α_D (ϕ,ψ = -90°, 180°), *trans*-amide α_D (ϕ,ψ = -90°, 180°), and *trans*-amide $C_{7\beta}$ (ϕ,ψ = -130°, 80°), with all remaining dihedral angles unrestrained during geometry optimization (**Figure 4b**, Fig. S115). The results showed a preference for χ_1, χ_2 near (-90°, +15°) in *cis*-amide structures, and a mixture of (-90°, +15°) and (+90°, +15°) preferences in *trans*-amide structures, consistent with similar work for related molecules.[25] Next, full backbone dihedral scans of ϕ and ψ angles (15° intervals) were performed starting from *cis*-amide and *trans*-amide isomers with -90° and +90° χ_1 angles, with all dihedral angles except ϕ and ψ unrestrained during optimization (Fig. S116). From these studies, the *cis*-amide energy minimum was found to be 1.26 kcal mol^{-1} lower than the *trans*-amide, in excellent

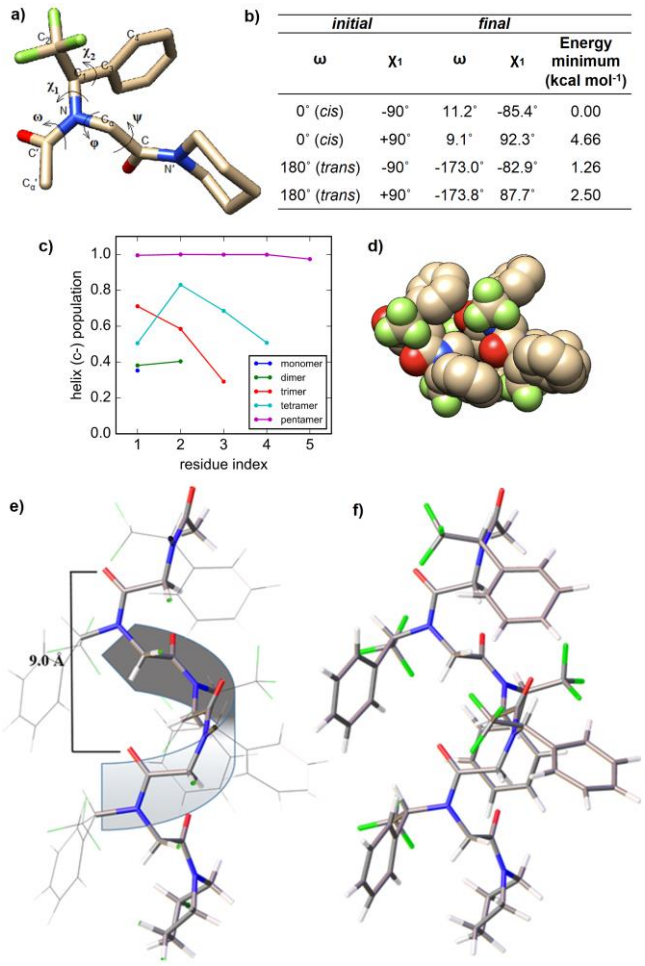

Figure 4. a) The lowest-energy conformation of **12**, annotated with dihedral angle definitions (see SI for details). **b**) Lowest-energy minima found in ϕ, ψ backbone dihedral scans started from *cis*- and *trans*-amide conformations with side-chain orientations χ1 = -90º and +90º. **c**) REMD simulations of oligomeric analogues of **12**, Ac-[N^{CF_3}Rpe]$_n$-Pip (n=1,2,3,4,5) showing an increasing preference to form right-handed *cis*-amide helices. **d**) Space-filling model of the predicted pentamer structure (n=5). **e-f**) Longitudinal views of a representative frame of the oligomer from the lowest temperature replica (300 K).

agreement with the experimental $K_{cis/trans}$ values measured (**Figure 2d**). In comparison, similar calculations for *N*Spe show a *cis*/*trans* energy minima gap of only 0.2 kcal mol^{-1}.[26] These results, in combination with the experiments above, strongly indicated that the single isomer seen experimentally corresponded to the *cis*-amide conformation.

The computed backbone dihedral (ϕ,ψ) landscape of **12** resembles that of the *N*Spe monomer,[25,26] but unlike *N*Spe, which favors a negative backbone ϕ-angle (near -90˚) by ~1 kcal mol^{-1} over the positive angle (near +90˚), **12** favors the *positive* angle by ~0.8 kcal mol^{-1} (Fig. S116). This may partly be due to unfavorable proximity (3.1 Å) of the carbonyl oxygen to the nearest fluorine in the electronegative CF_3 group for the *cis*-amide negative ϕ-angle conformation (5.2 Å for the positive ϕ-angle conformation).

Comparative analysis of model systems **1, 9, 10, 11** and **12** using natural bond orbital (NBO) analysis (see SI for details)

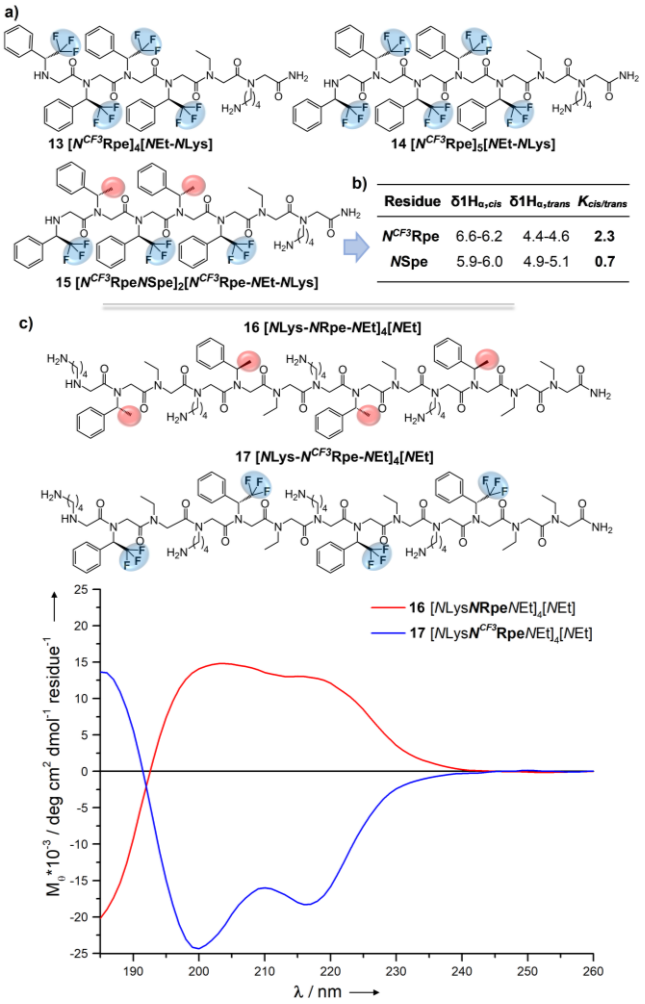

Figure 5. a) Structure of peptoid oligomers **13-15**. **b**) Main ^{1}H-NMR parameters of *N*Spe and N^{CF_3}Rpe residues as analyzed in **15**. **c**) Structure and average CD spectra (n=3) of peptoid hetero-oligomers **13** (shown in red) and **14** (shown in blue). All measurements in CH_3CN.

suggests the presence of $n\longrightarrow\pi^*$effects, as seen by a decrease in the natural charge of the carbonyl oxygen atom and increase in the total π^* occupancy of the aromatic system. The extent of these effects is strongly correlated with the experimental $K_{cis/trans}$ ratios, and are most significant for system **10**. These effects are less significant for system **12**, supporting a mechanism of *cis*-isomer stabilization in **12** in which a combination of inductive and steric factors, rather than $n\longrightarrow\pi^*$ interactions *per se*, act to achieve such a large $K_{cis/trans}$ ratio. This result also agrees with the orientation of the carbonyl and aromatic groups in the minimum energy structure of **12**.

To predict the conformational preferences of N^{CF_3}Rpe oligomers, we performed replica exchange molecular dynamics (REMD) simulations[26,27] of **12** as well as the related oligomeric species Ac-[N^{CF_3}Rpe]$_n$-Pip, for n = 1,2,3,4,5. (**Figure 4c**). The simulations agreed with QM studies (Table S6), with *cis*-amide populations above 95% for all residues (Fig. S117). Strikingly, simulations also predicted that larger oligomers are increasingly prone to form stable right-handed helices (e.g. negative ϕ-angle), with N^{CF_3}Rpe pentamers displaying *cis*-amide helix populations of nearly 100% (**Figure 4c-f**). These results likely stem from the large $K_{cis/trans}$ value for **12**,

which is additionally rewarded by the excellent side-chain packing achieved in the helical conformation. The difference between the ϕ-angles seen in the model (**12**) and the N^{CF_3}Rpe oligomers we believe arises due to **12** being unconstrained by the side chain packing that is present within the oligomers.[12,14]

The REMD simulations were experimentally validated by ^{19}F-NMR (Fig. S126) and circular dichroism (CD) (Fig. S140) analysis of oligomers **13**-**15** (**Figure 5**). By comparison of **13** and **14** it can be seen that increasing the number of sequential N^{CF_3}Rpe residues leads to an increase in the conformational homogeneity. Similarly, removal of N^{CF_3}Rpe residues from the sequence (e.g. **14** versus **15**) leads to a decrease in conformational homogeneity. In addition, HSQC-TOCSY and NOESY analysis of peptoid **14** demonstrated the enhanced *cis*-amide preference of the N^{CF_3}Rpe residues ($K_{cis/trans}$= 2.3) compared to the *N*Spe ($K_{cis/trans}$= 0.7) (**Figure 5b**; Figs. S127 and S130). To further explore the application of N^{CF_3}Rpe as a tool to stabilize the helical conformation of longer peptoids two model hetero-oligomers were prepared (**16** and **17**, **Figure 5c**). When the secondary structures of **16** and **17** were analyzed by CD clear differences beyond the opposing helical chirality enforced by both monomers (e.g. left-hand helix for *N*Rpe and a right-handed helix for N^{CF_3}Rpe) were seen. Specifically, **17** showed a dramatic 42% increase in the $M_{\theta,218}$ compared to **16**. This result provides clear evidence that the substitution of non-fluorinated *N*Rpe residues by their α-trifluoromethyl analogues (N^{CF_3}Rpe) offers a route to enhance the peptoid secondary helical structure.

In summary, we report the application of fluorine as a tool to design monomers which enhance the conformational stability of α-peptoids. The $K_{cis/trans}$ values recorded for the N^{4f}pym containing di-peptoid **10** are among the largest ever reported for a non-chiral monomer. N^{4f}pym also represents the first example of a non-chiral, non-charged aromatic monomer that can induce a strong *cis*-amide preference. The N^{4f}pym residue achieves its high $K_{cis/trans}$ values by pushing the electronic $n\rightarrow\pi^*$ effects to the limit of what is possible in a neutral system. We recently reported the application of fluorine inductive/ di-polar effects as a new tool to modulate $K_{cis/trans}$ ratios[23] but the N^{CF_3}Rpe monomer demonstrates the benefits of combining fluorine induced steric and fluorine induced inductive electronic effects. Indeed, as evidenced by NMR analysis, *ab initio* and molecular dynamics calculations, the N^{CF_3}Rpe monomer has the ability to push the $K_{cis/trans}$ equilibrium to essentially favor one single isomer. REMD simulations of N^{CF_3}Rpe oligomers predicted the formation of highly stable right-handed helices and this was experimentally validated *via* preparation and conformational analysis of a series of N^{CF_3}Rpe containing peptoid oligomers. N^{4f}pym and N^{CF_3}Rpe provide a much-needed expansion of the limited tool-box of monomers available for the rational design of conformationally stable peptoids.

ASSOCIATED CONTENT

Supporting Information

The Supporting Information is available free of charge on the ACS Publications website. This material includes: Experimental procedures and characterization data for peptoid monomers **1**, **9**-**12** and oligomers **13**-**17** (PDF). X-ray crystallographic data for by-product from **12** (CIF).

AUTHOR INFORMATION

Corresponding Authors

* s.l.cobb@durham.ac.uk; voelz@temple.edu

Author Contributions

The manuscript was written with contributions from all authors who have given their approval to the final submitted version.

ACKNOWLEDGMENTS

We thank Graham E. Dobereiner for expertise with Natural Bond Orbital calculations. This work was financially supported by the Initial Training Network, FLUOR21, funded by the FP7 Marie Curie Actions of the European Commission (FP7-PEOPLE-2013-ITN-607787). In addition, V.A.V., G.Z. and M.H. were supported by National Institutes of Health (NIH) grant 1R01GM123296. This research includes calculations performed on Temple University's HPC resources partially supported by the National Science Foundation through MRI grant 1625061 and by the US Army Research Laboratory under contract number W911NF-16-2-0189.

REFERENCES

(1) Luo, Y.; Bolt, H. L.; Eggimann, G. A.; McAuley, D. F.; McMullan, R.; Curran, T.; Zhou, M.; Jahoda, P. C. A. B.; Cobb, S. L.; Lundy, F. T. Peptoid Efficacy against Polymicrobial Biofilms Determined by Using Propidium Monoazide-Modified Quantitative PCR. *ChemBioChem* **2017**, *18* (1), 111–118

(2) Sanborn, T. J.; Wu, C. W.; Zuckermann, R. N.; Barron, A. E. Extreme stability of helices formed by water-soluble poly-N-substituted glycines (polypeptoids) with α-chiral side chains. *Biopolymers* **2002**, *63* (1), 12–20.

(3) Eggimann, G. A.; Bolt, H. L.; Denny, P. W.; Cobb, S. L. Investigating the Anti-leishmanial Effects of Linear Peptoids. *ChemMedChem* **2015**, *10* (2), 233–237

(4) Chongsiriwatana, N. P.; Patch, J. A.; Czyzewski, A. M.; Dohm, M. T.; Ivankin, A.; Gidalevitz, D.; Zuckermann, R. N.; Barron, A. E. Peptoids that mimic the structure, function, and mechanism of helical antimicrobial peptides. *Proc. Natl. Acad. Sci.* **2008**, *105* (8), 2794–2799.

(5) Hara, T.; Durell, S. R.; Myers, M. C.; Appella, D. H. Probing the Structural Requirements of Peptoids That Inhibit HDM2–p53 Interactions. *J. Am. Chem. Soc.* **2006**, *128* (6), 1995–2004.

(6) Trader, D. J.; Simanski, S.; Kodadek, T. A Reversible and Highly Selective Inhibitor of the Proteasomal Ubiquitin Receptor Rpn13 Is Toxic to Multiple Myeloma Cells. *J. Am. Chem. Soc.* **2015**, *137* (19), 6312–6319.

(7) Reddy, M. M.; Wilson, R.; Wilson, J.; Connell, S.; Gocke, A.; Hynan, L.; German, D.; Kodadek, T. Identification of Candidate IgG Biomarkers for Alzheimer's Disease via Combinatorial Library Screening. *Cell* **2011**, *144* (1), 132–142.

(8) Zhao, Z.; Zhu, L.; Bu, X.; Ma, H.; Yang, S.; Yang, Y.; Hu, Z. Label-free detection of Alzheimer's disease through the ADP3 peptoid recognizing the serum amyloid-beta42 peptide. *Chem Commun* **2015**, *51* (4), 718–721.

(9) (a) Lee, B.-C.; Chu, T. K.; Dill, K. A.; Zuckermann, R. N. Biomimetic Nanostructures: Creating a High-Affinity Zinc-Binding Site in a Folded Nonbiological Polymer. *J. Am. Chem. Soc.* **2008**, *130* (27), 8847–8855. (b) Reddy, M. M.; Kodadek, T. Protein "fingerprinting" in complex mixtures with peptoid microarrays. *Proc. Natl. Acad. Sci. U. S. A.* **2005**, *102* (36), 12672–12677. (c) Knight, A. S.; Zhou, E. Y.; Pelton, J. G.; Francis, M. B. Selective Chromium(VI) Ligands Identified Using Combinatorial Peptoid Libraries. *J. Am. Chem. Soc.* **2013**, *135*(46), 17488–17493. (c) Baskin, M.; Maayan, G. A rationally designed metal-binding helical peptoid for selective recognition processes. *Chem Sci.* **2016**, *7* (4), 2809–2820. (d) Pirrung, M. C.; Park, K.; Tumey, L. N. ^{19}F-

Encoded Combinatorial Libraries: Discovery of Selective Metal Binding and Catalytic Peptoids. *J. Comb. Chem.* **2002**, *4* (4), 329–344. (e) Maayan, G.; Ward, M. D.; Kirshenbaum, K. Folded biomimetic oligomers for enantioselective catalysis. *Proc. Natl. Acad. Sci.* **2009**, *106* (33), 13679–13684.

(10) Armand, P.; Kirshenbaum, K.; Goldsmith, R. A.; Farr-Jones, S.; Barron, A. E.; Truong, K. T.; Dill, K. A.; Mierke, D. F.; Cohen, F. E.; Zuckermann, R. N.; Bradley E. K. NMR determination of the major solution conformation of a peptoid pentamer with chiral side chains. *Proc. Natl. Acad. Sci.* **1998**, *95* (8), 4309–4314.

(11) Murnen, H. K.; Rosales, A. M.; Jaworski, J. N.; Segalman, R. A.; Zuckermann, R. N. Hierarchical Self-Assembly of a Biomimetic Diblock Copolypeptoid into Homochiral Superhelices. *J. Am. Chem. Soc.* **2010**, *132* (45), 16112–16119.

(12) Stringer, J. R.; Crapster, J. A.; Guzei, I. A.; Blackwell, H. E. Extraordinarily Robust Polyproline Type I Peptoid Helices Generated *via* the Incorporation of α-Chiral Aromatic *N*-1-Naphthylethyl Side Chains. *J. Am. Chem. Soc.* **2011**, *133* (39), 15559–15567.

(13) (a) Gorske, B. C.; Mumford, E. M.; Gerrity, C. G.; Ko, I. A Peptoid Square Helix via Synergistic Control of Backbone Dihedral Angles. *J. Am. Chem. Soc.* **2017**, *139* (24), 8070–8073. (b) Roy, O.; Dumonteil, G.; Faure, S.; Jouffret, L., Kriznik, A.; Taillefumier, C. Highly homogeneous and robust PolyProline type I helices from peptoids with non-aromatic α-chiral side chains. *J. Am. Chem. Soc.* **2017**, *139* (38), 13533–13540.

(14) Crapster, J. A.; Guzei, I. A.; Blackwell, H. E. A Peptoid Ribbon Secondary Structure. *Angew. Chem. Int. Ed.* **2013**, *52* (19), 5079–5084.

(15) Huang, K.; Wu, C. W.; Sanborn, T. J.; Patch, J. A.; Kirshenbaum, K.; Zuckermann, R. N.; Barron, A. E.; Radhakrishnan, I. A Threaded Loop Conformation Adopted by a Family of Peptoid Nonamers. *J. Am. Chem. Soc.* **2006**, *128* (5), 1733–1738.

(16) Mannige, R. V.; Haxton, T. K.; Proulx, C.; Robertson, E. J.; Battigelli, A.; Butterfoss, G. L.; Zuckermann, R. N.; Whitelam, S. Peptoid nanosheets exhibit a new secondary-structure motif. *Nature* **2015**, *526* (7573), 415–420.

(17) Nam, K. T.; Shelby, S. A.; Choi, P. H.; Marciel, A. B.; Chen, R.; Tan, L.; Chu, T. K.; Mesch, R. A.; Lee, B.-C.; Connolly, M. D.; Kisielowski, C.; Zuckermann R. N. Free-floating ultrathin two-dimensional crystals from sequence-specific peptoid polymers. *Nat. Mater.* **2010**, *9* (5), 454–460.

(18) Armand, P.; Kirshenbaum, K.; Falicov, A.; Dunbrack, R. L.; Dill, K. A.; Zuckermann, R. N.; Cohen, F. E. Chiral N-substituted glycines can form stable helical conformations. *Fold. Des.* **1997**, *2* (6), 369–375.

(19) Gorske, B. C.; Blackwell, H. E. Tuning Peptoid Secondary Structure with Pentafluoroaromatic Functionality: A New Design Paradigm for the Construction of Discretely Folded Peptoid Structures. *J. Am. Chem. Soc.* **2006**, *128* (44), 14378–14387.

(20) Gorske, B. C.; Bastian, B. L.; Geske, G. D.; Blackwell, H. E. Local and Tunable n→π* Interactions Regulate Amide Isomerism in the Peptoid Backbone. *J. Am. Chem. Soc.* **2007**, *129* (29), 8928–8929.

(21) Gorske, B. C.; Stringer, J. R.; Bastian, B. L.; Fowler, S. A.; Blackwell, H. E. New Strategies for the Design of Folded Peptoids Revealed by a Survey of Noncovalent Interactions in Model Systems. *J. Am. Chem. Soc.* **2009**, *131* (45), 16555–16567.

(22) Aliouat, H.; Caumes, C.; Roy, O.; Zouikri, M.; Taillefumier, C.; Faure, S. 1,2,3-Triazolium-Based Peptoid Oligomers. *J. Org. Chem.* **2017**, *82* (5), 2386–2398.

(23) Gimenez, D.; Aguilar, J. A.; Bromley, E. H. C.; Cobb, S. L. *Angew. Chem. Int. Ed.* **2018**, *57* (33), 10549–10553.

(24) Sui, Q.; Borchardt, D.; Rabenstein, D. L. Kinetics and Equilibria of Cis/Trans Isomerization of Backbone Amide Bonds in Peptoids. *J. Am. Chem. Soc.* **2007**, *129* (39), 12042–12048.

(25) Butterfoss, G. L.; Renfrew, P. D.; Kuhlman, B.; Kirshenbaum, K.; Bonneau, R. A Preliminary Survey of the Peptoid Folding Landscape. *J. Am. Chem. Soc.* **2009**, *131* (46), 16798–16807.

(26) Mukherjee, S.; Zhou, G.; Michel, C.; Voelz, V. A. Insights into Peptoid Helix Folding Cooperativity from an Improved Backbone Potential. *J. Phys. Chem. B* **2015**, *119* (50), 15407–15417.

(27) Voelz, V. A.; Dill, K. A.; Chorny, I. Peptoid conformational free energy landscapes from implicit-solvent molecular simulations in AMBER. *Biopolymers* **2011**, *96* (5), 639–650.

TOC

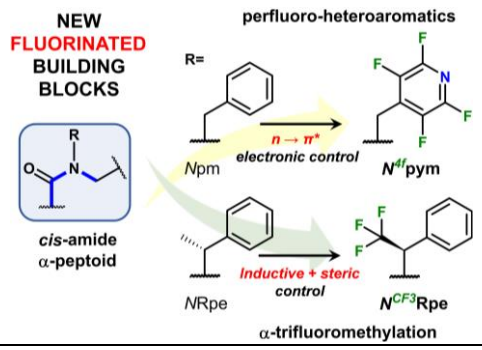
NEW
FLUORINATED
BUILDING
BLOCKS
cis-amide
α-peptoid
perfluoro-heteroaromatics
R=
Npm
n → π*
electronic control
N4fpym
NRpe
Inductive + steric
control
NCF3Rpe
α-trifluoromethylation